



HAL
open science

Influence of the position of ionic groups in amphoteric polyelectrolytes on hydration and ionic conduction: Side chain vs main chain

Riccardo Narducci, Emanuela Sgreccia, Gianfranco Ercolani, Marco Sette, Simonetta Antonaroli, Luca Pasquini, Philippe Knauth, Maria Luisa Di Vona

► To cite this version:

Riccardo Narducci, Emanuela Sgreccia, Gianfranco Ercolani, Marco Sette, Simonetta Antonaroli, et al.. Influence of the position of ionic groups in amphoteric polyelectrolytes on hydration and ionic conduction: Side chain vs main chain. *European Polymer Journal*, 2019, 119 (5), pp.45-51. 10.1016/j.eurpolymj.2019.07.001 . hal-02658017

HAL Id: hal-02658017

<https://amu.hal.science/hal-02658017>

Submitted on 30 May 2020

HAL is a multi-disciplinary open access archive for the deposit and dissemination of scientific research documents, whether they are published or not. The documents may come from teaching and research institutions in France or abroad, or from public or private research centers.

L'archive ouverte pluridisciplinaire **HAL**, est destinée au dépôt et à la diffusion de documents scientifiques de niveau recherche, publiés ou non, émanant des établissements d'enseignement et de recherche français ou étrangers, des laboratoires publics ou privés.



Distributed under a Creative Commons Attribution - NonCommercial - NoDerivatives 4.0 International License



Influence of the position of ionic groups in amphoteric polyelectrolytes on hydration and ionic conduction: Side chain vs main chain

Riccardo Narducci^a, Emanuela Sgreccia^a, Gianfranco Ercolani^b, Marco Sette^b,
Simonetta Antonaroli^b, Luca Pasquini^c, Philippe Knauth^c, Maria Luisa Di Vona^{a,*}

^a University of Rome Tor Vergata, Dep. Industrial Engineering and International Associated Laboratory: Ionomer Materials for Energy, 00133 Roma, Italy

^b University of Rome Tor Vergata, Dep. Chemical Sciences and Technologies, 00133 Roma, Italy

^c Aix Marseille Univ, CNRS, MADIREL (UMR 7246) and International Associated Laboratory: Ionomer Materials for Energy, Campus St Jérôme, 13013 Marseille, France

ARTICLE INFO

Keywords:

Poly(sulfone)
Ionomers
pH-dependent properties
Smart polymers

ABSTRACT

Amphoteric ionomers were synthesized with two different approaches to study the influence of a flexible side chain containing the functional groups vs grafting of the functional groups directly on the main chain. Poly(sulfone) was functionalized with 6-aminohexanoic acid (ANF-1) or by successive carboxylation and amination of the aromatic main chain (ANF-2). The samples were characterized by FTIR and NMR spectroscopies and thermogravimetric analysis. Acid and base constants were measured by titration. We also determined the hydration and the ionic conductivity for acid, base and zwitterionic forms made by variation of the pH.

The basic forms containing dissociated carboxylic groups and mobile cations showed a higher water uptake and a higher conductivity. The zwitterionic forms presented a low water uptake for both polyelectrolytes and the lowest conductivity for ANF-2. The reduced conductivity in acidic conditions of ANF-1, where amine groups were protonated and only anions were mobile, was related to the position of ammonium moieties inside the side chain. This work showed how the properties of stimuli-responsive polymers depended on the position of the functional groups.

1. Introduction

Ion exchange polymers [1,2] are fascinating materials with a wide variety of applications, ranging from water purification [3,4], sensors and actuators, non-linear optics [5], biomedical processing [5] to energy storage and conversion [6–9]. The most prominent ion exchange groups are sulfonic acid for cation exchangers [10–13] and quaternary ammonium groups for anion exchangers [14–16]. Amphoteric ionomer materials contain simultaneously grafted anionic and cationic groups on the macromolecule. The zwitterionic form is obtained when the amount of positive and negative charges is balanced (isoelectric point) [5].

A very attractive feature of amphoteric ion-exchange polymers is the possibility to control properties related to the ionic charge by changing the external pH. This allows designing smart stimulus-responsive soft materials with controlled property dependence [17]. The consequent activity as anti-fouling materials, preventing adsorption of organic and biological macromolecules on the surface, [18] is another important advantage of amphoteric polyelectrolytes. Different fields can benefit of their use, such as high performance actuators [19], drug

and protein separation [20–22], hemodialysis membranes [23,24], electrolyte purification by nanofiltration [25], piezodialysis [26], and water splitting [27,28].

The hydration [29] and ionic conductivity [30] of amphoteric polymers are particularly sensitive to variations of pH, related to a variable density of charged ionic groups. Permselectivity [31] can also be modulated by change of the Donnan potential [1], corresponding to an excess of positive or negative ionic charges grafted on the polymer chain. We found a particularly low ion permeability for ampholytic polymers [3,32].

Amphoteric polymers are prepared by various methods, including copolymerization of different polymers, radiation grafting [33], blending of acidic and basic polymers or the assembling of different layers. We prepared amphoteric ionomers by innovative synthesis methods, introducing sulfonic acid and sulfonamide groups into poly(ether ether ketone) [30] or carboxylic and amine groups grafted to a cross-linkable silica network into polysulfone [34].

In this work, polysulfone (PSU) was functionalized in order to produce amphoteric polymers, where the ionic groups, carboxylic acid and alkyl amine, were linked to the main chain or placed on a long side

* Corresponding author.

E-mail address: divona@uniroma2.it (M.L. Di Vona).

<https://doi.org/10.1016/j.eurpolymj.2019.07.001>

Received 5 May 2019; Received in revised form 24 June 2019; Accepted 1 July 2019

Available online 02 July 2019

0014-3057/ © 2019 The Authors. Published by Elsevier Ltd. This is an open access article under the CC BY-NC-ND license

(<http://creativecommons.org/licenses/by-nc-nd/4.0/>).

chain. This procedure allowed tailoring the ion exchange capacity, but it should also modify the hydrophilic-hydrophobic nanophase separation and, consequently, hydration and ionic conduction, as shown recently in other ion exchange membranes [35–36]. For a direct substitution on the main chain, we used carboxylation by CO₂ followed by chloromethylation and reaction with trimethylamine. For long side chain functionalization, we applied the chloromethylation route with direct reaction with 6-aminohexanoic acid.

2. Experimental

2.1. Materials

Polysulfone (PSU) was purchased from UDEL Co. 6-Aminohexanoic acid (6AHA) and all other products were obtained from Aldrich and used without further purification.

2.2. Synthesis procedures

2.2.1. Chloromethylated polysulfone

Chloromethylated polysulfone (PSU-CH₂Cl) was synthesized from PSU following the procedure reported elsewhere [37,38]. The chloromethylation degree was DCM = 0.7.

2.2.2. ANF-1: Introduction of –CO₂H and –NR₂ groups by chloromethylation and substitution with an amino acid

Dried PSU-CH₂Cl (2 g, 4.2 meq) was dissolved at RT under N₂ in anhydrous DMSO. KI and K₂CO₃ were added with a molar ratio PSU-CH₂Cl:KI:K₂CO₃ 1:1:3. The mixture was kept under stirring for 1 h, then 6-aminohexanoic acid (PSU-CH₂Cl : 6-AHA 1:3) was slowly added and the reaction was kept at 70 °C for 3 days. The yellow mixture was precipitated in ethanol, washed in deionized water and ethanol to remove the residual salts. The white powder was dried at 65 °C for 3 days.

¹H NMR (DMSO-*d*₆, acid form: PSU-CH₂-NH₂⁺-CH₂CH₂CH₂CH₂CH₂-CO₂H) δ = 1.0 (NCH₂CH₂CH₂CH₂CH₂-CO₂H, m), δ = 1.5 (NCH₂CH₂CH₂CH₂CH₂-CO₂H, m), δ = 1.6 (CH₃-PSU, 6H), δ = 1.9 (NCH₂CH₂CH₂CH₂CH₂-CO₂H, m), δ = 2.3 (NCH₂CH₂CH₂CH₂CH₂-CO₂H, t), δ = 2.6 (NCH₂CH₂CH₂CH₂CH₂-CO₂H, t), δ = 4.2 (PSU-CH₂-NH₂⁺, s, 1.14H), δ = 6.75–8.25 (PSU aromatic region). The degree of functionalization was measured by comparison between of the area of PSU-CH₂-NH₂⁺ groups and PSU methyl groups and was 0.57.

Membranes of ANF-1 were obtained using N-methylpyrrolidone (NMP) as solvent. Typically, 200 mg ANF-1 were dissolved in 10 mL NMP under stirring. The solvent was evaporated by heating the solution in a Petri dish in an oven at 90 °C for 24 h.

2.2.3. ANF-2: Introduction of –CO₂H and –NR₂ groups by carboxylation and amination

2.2.3.1. Carboxylation of PSU. After drying over night at 120 °C, PSU (5 g, 11.3 meq) was dissolved at RT in anhydrous THF (100 mL) under nitrogen flux. The resulting solution (concentration 5%) was cooled to –50 °C, then *n*-butyllithium (2.5 M in hexane, 9.0 meq, 3.6 mL) was slowly added by a self-balancing funnel. During this time, the colour of the solution changed from uncoloured to red-brown. After 1 h, some blocks of dry ice were added while the solution was kept under vigorous stirring. The resulting white solution was slowly warmed to RT and let standing over night. Carboxylated PSU was precipitated and washed in 2-propanol and then dried at 60 °C for one night.

2.2.3.2. Esterification. The basic form of carboxylated PSU (2.0 g, 4.14 meq) was dissolved in DMSO (20 mL), then iodomethane (0.52 mL, 8.28 meq) was added in two times every 30 min. The reaction was kept at 80 °C for 1 h. The formed ester was recovered by precipitating the hot solution in methanol, heating in fresh methanol and then washing in boiling water.

¹H NMR (CDCl₃, PSU-CO₂CH₃) δ = 1.6 (CH₃-PSU, 6H), δ = 3.9 (CH₃O, 2.4H), δ = 6.75–8.25 (PSU aromatic region). The degree of carboxylation (DCA) was measured by comparison between of the area of methyl ester and PSU methyl groups and was DCA = 0.80.

2.2.3.3. Chloromethylation of carboxylated and esterificated PSU. Carboxyl methyl ester PSU (PSU-CO₂CH₃ 1.9 g, 4.24 meq), dried during one night, was dissolved in chloroform (200 mL) at RT under N₂. After dissolution, (CH₂O)_n (1.14 g) and Me₃SiCl (4.85 mL) were added. SnCl₄ (0.09 mL in 30 mL of chloroform) was then slowly introduced in two times every 24 h. The solution was stirred under nitrogen flux at 70 °C one week. The ratio PSU-CO₂CH₃:(CH₂O)_n:Me₃SiCl:SnCl₄ was 5:50:50:1. The product was precipitated in methanol. Solubility tests showed that the sample dissolved in CHCl₃ and in DMSO.

¹H NMR (CDCl₃, PSU-(CO₂CH₃)CH₂Cl) δ = 1.6 (CH₃-PSU, 6H), δ = 3.9 (CH₃O, 2.4H), δ = 4.5 (CH₂Cl, 1.4H), δ = 6.75–8.25 (PSU aromatic region). The degree of chloromethylation was measured by comparison between of the area of chloromethyl moiety and PSU methyl groups and was DCM = 0.70.

2.2.3.4. Amination of chloromethylated and esterificated PSU. The chloromethylated and carboxylated methyl ester sample (PSU-(CO₂CH₃)CH₂Cl, 1.07 g, 2.1 meq) was dissolved in DMSO (40 mL) under N₂ at 70 °C. Potassium carbonate and dimethylamine (2 M solution in THF) were then added with a reagent ratio PSU-(CO₂CH₃)CH₂Cl:K₂CO₃:DMA = 1:2:1.2. The solution was kept under stirring one week. The aminated sample was precipitated in water.

2.2.3.5. Hydrolysis of carboxylated methyl ester (ANF-2). The previous sample was dissolved in DMSO at 100 °C under stirring and a 2 M NaOH solution was then added very slowly. After 1 h the solution was cooled to RT and 1 M HCl solution was added until pH = 7. The amphoteric polymer was precipitated and washed in water and then dried in the oven at 70 °C for 2 days.

The polymer showed a low solubility in DMSO, NMP and other solvents and membranes cast by these solvents were very brittle.

¹H NMR (DMSO-*d*₆, acid form: PSU-(CO₂H)CH₂N⁺H(CH₃)₂) δ = 1.6 (CH₃-PSU, 6H), δ = 3.3 (CH₃-N⁺, 4.2H), δ = 4.3 (PSU-CH₂N⁺, 1.4H), δ = 6.75–8.25 (PSU aromatic region). The degree of amination (DAM) was measured by comparison between the area of methylamino groups and PSU methyl groups and was DAM = 0.7. The obtained ratio of CO₂H to NR₂ functional groups was 1.1.

2.3. Characterizations

2.3.1. NMR analysis

¹H NMR spectra were recorded with a Bruker AVANCE III spectrometer operating at 400 MHz. DMSO-*d*₆ and CDCl₃ were used as solvents. Chemical shifts (ppm) were referenced to tetramethylsilane (TMS).

Heteronuclear Single Quantum Spectrum (HSQC) was collected with the standard Bruker sequence (hsqcetgp). Spectra were processed by using a squared sine bell and polynomial baseline correction. Spectral assignments were performed by using spectral simulation performed with MNova (Mestrelab Research, Spain) in conjunction with experimental data.

2.3.2. FTIR

FTIR spectra were recorded in transmission mode in the range of 4000–400 cm^{–1} using a spectrometer Perkin-Elmer Spectrum 100. The samples were analysed in cesium iodide cells. Spectra were normalized against a background spectrum.

2.3.3. High-resolution thermogravimetry

The thermal degradation of the polymers was investigated by high resolution thermogravimetric analysis (TGA Q500, TA Instruments),

performed between 25 and 550 °C with a maximum heating rate of 3 °C/min under air flux in platinum sample holders.

2.3.4. Acid, basic, and zwitterionic forms; titration

Acid, basic, and zwitterionic forms of the two amphoteric ionomers were obtained by immersion of the powders in solutions with fixed pH values.

The acid form was made under stirring in 2 M HCl during 24 h. The samples were filtered, washed several times with deionized water and dried at 60 °C and over P₂O₅. For the determination of the acid and base constants and the isoelectric points, the dry samples were potentiometrically titrated with 0.022 M NaOH under nitrogen. The pH values were measured after equilibration of the mixture, which can take up to 24 h.

The total ion exchange capacity (IEC) was obtained by back-titration. The basic form was prepared by immersion under stirring in 2 M NaOH during 24 h. The samples were repeatedly washed with water and placed in 5 mL of 0.1 M HCl for 24 h. The solution was back-titrated with 0.02 M NaOH. The zwitterionic forms were made by immersion in a solution with the pH of the isoelectric point.

2.3.5. Hydration measurements

The water uptake (WU) was measured at 25 °C on powder samples exposed 7 days at 100% RH. The wet mass (m_{wet}) was determined by rapid weighing of the sample in a closed vessel. The dry mass was measured after drying the sample over P₂O₅ for 24 h (m_{dry}).

The WU was calculated from the equation:

$$WU/\% = 100 \cdot \frac{(m_{\text{wet}} - m_{\text{dry}})}{m_{\text{dry}}} \quad (1)$$

2.3.6. Conductivity measurements

The through-plane ionic conductivity was determined between 25 and 80 °C by electrochemical impedance spectroscopy (EIS) in fully humidified conditions using a Parstat 4000 instrument. The ac voltage amplitude was 20 mV and the frequency range was between 10 Hz and 6 MHz. Swagelok cells with cylindrical stainless steel electrodes of 6 mm diameter were used.

Measurements were performed on sample membranes and sample pellets, which were compressed from powders under 1 MPa pressure at room temperature. The through-plane resistance of the samples R_{mat} was determined from a non-linear least-square fitting of Nyquist plots using the Zfit program. The ionic conductivity σ was calculated according to the equation:

$$\sigma = \frac{d}{R_{\text{mat}} \cdot A} \quad (2)$$

where d was the sample thickness and $A = 0.28 \text{ cm}^2$ the electrode area.

3. Results and discussion

3.1. Synthesis of ANF-1 and ANF-2

The synthetic route for the preparation of ANF-1 is reported in Fig. 1. It was possible to obtain the γ -amino acid derivative of PSU in one-step, starting from the chloromethylated polymer. This simple strategy allowed the formation of amphoteric ionomers bearing the acid and basic groups in the same repeat unit and chain. The reaction occurred via a S_N2 mechanism in the presence of KI. Iodide ions acted as a nucleophile on the chloromethyl derivative, generating a more reactive alkyl iodide that reacted faster with the primary amine.

PSU was chloromethylated using paraformaldehyde and chlorotrimethylsilane in the presence of a homogeneous Lewis acid catalyst SnCl₄; these synthesis conditions avoided the use of toxic chloromethylating agents [37,39].

This approach allowed obtaining an exact balance between acid and basic groups in the amphoteric ionomer.

The synthesis of ANF-2 is reported in Fig. 2. The first step was a hydrogen metal exchange reaction with the formation of an organolithium compound followed by an electrophilic attack of carbon dioxide.

The metalation reactions are particularly suitable when the organometallic species are stabilized by resonance; sulfone groups on the PSU backbone, which are electron-withdrawing by mesomeric effect, stabilized and directed the lithiation in the *ortho* position [40–42].

The ratio PSU/BuLi was 0.8, in order to obtain a degree of carboxylation DCA = 0.8, as reported by Guiver et al. [43]. The methyl esterification was performed on carboxylated PSU in order to increase the polymer solubility and to protect the CO₂H group during the following steps. The degree of carboxylation measured by ¹H NMR was indeed DCA = 0.8. The methyl ester derivative of carboxylated PSU was chloromethylated as previously described for the synthesis of ANF-1. The chloromethylated derivative was aminated with dimethylamine via a S_N2 mechanism in the presence of K₂CO₃, which was helpful to trap the hydrochloric acid formed during the reaction. After hydrolysis, the compound ANF-2 was obtained.

The FTIR spectra of ANF-1 and ANF-2 are shown in Fig. 3 below 1800 cm⁻¹, where the most important peaks are observed.

Typical PSU absorption peaks [16] were present in both ANF-1 and ANF-2 spectra. Carboxylic acid groups were visible for the amphoteric samples around 1720 cm⁻¹ (C=O stretch), while the peak at 1630 cm⁻¹, present only in ANF-1 polymer, was due to the N–H bending of the secondary amine [44]. Bands at 1485 cm⁻¹ were ascribed to the scissoring of CH₂ and CH₃ moieties enhanced by the skeletal vibration of aromatic hydrocarbons that was visible as a shoulder around 1460 cm⁻¹. The absorption at 1230 cm⁻¹ was attributed to the C–N stretch that overlapped with the asym vibration of the ether linkage in the PSU matrix [45]. The peak at 1050 cm⁻¹ was assigned to trisubstituted benzene [46].

The ¹H NMR attribution of ANF-1 and ANF-2 are reported in the Experimental section. Fig. 4 shows the ¹H–¹³C HSQC spectra of ANF-2 with underlined correlation between the peaks.

The hetero-correlation ¹H–¹³C (Fig. 4) showing the coupling especially between the nitrogen and the benzylic moiety confirmed the structure of ANF-2.

3.2. Determination of acidic and basic constants

ANF-1 and ANF-2 powders were titrated starting from the acid form, made by immersion in 1 M HCl for 2 days.

Fig. 5 shows the titration curve of ANF-1. After reaction with acid, the backbone showed an excess positive charge corresponding to the protonation of the secondary amine. The inflection point in the titration curve corresponded to the complete neutralization of the carboxylic acid, which was equivalent to the isoelectric point: the number of positive (ammonium) and negative charges (carboxylate) was equivalent. From the curve (Fig. 5) resulted an isoelectric point pI = pH = 7.4.

The relation between the isoelectric point and the acid constants of the carboxylic (K_{a1}) and ammonium (K_{a2}) groups was written [47]:

$$pI = \frac{pK_{a1} + pK_{a2}}{2} \quad (3)$$

The acid constant of the carboxylic acid was read from the pH at half neutralization: pK_{a1} = 5.7. According to Eq. (3), the acid constant of the ammonium group was pK_{a2} = 9.1. The pH at half-neutralization of the ammonium group (Fig. 5) gave pK_{a2} = 9.0, in good agreement with the previous value.

The total IEC was obtained by back-titration with NaOH. The IEC = 0.98 meq/g corresponded to a degree of functionalization = 0.51 in good agreement with the NMR result (0.57). Given the initial chloromethylation degree of 0.7 (see experimental), the conversion

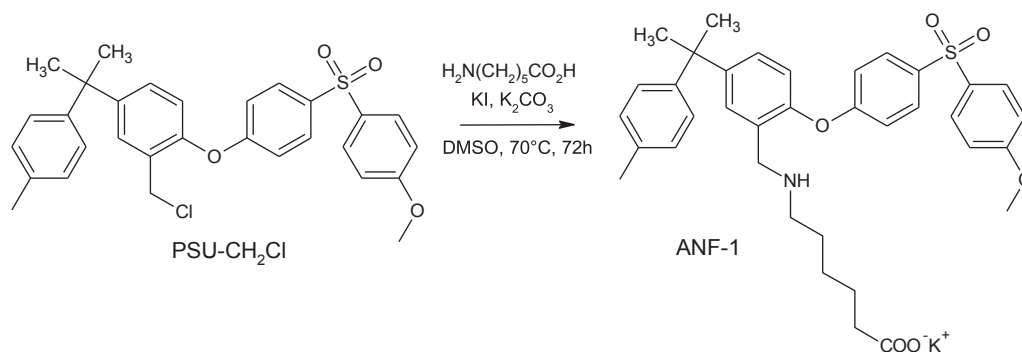


Fig. 1. Reaction pathway for the synthesis of ANF-1.

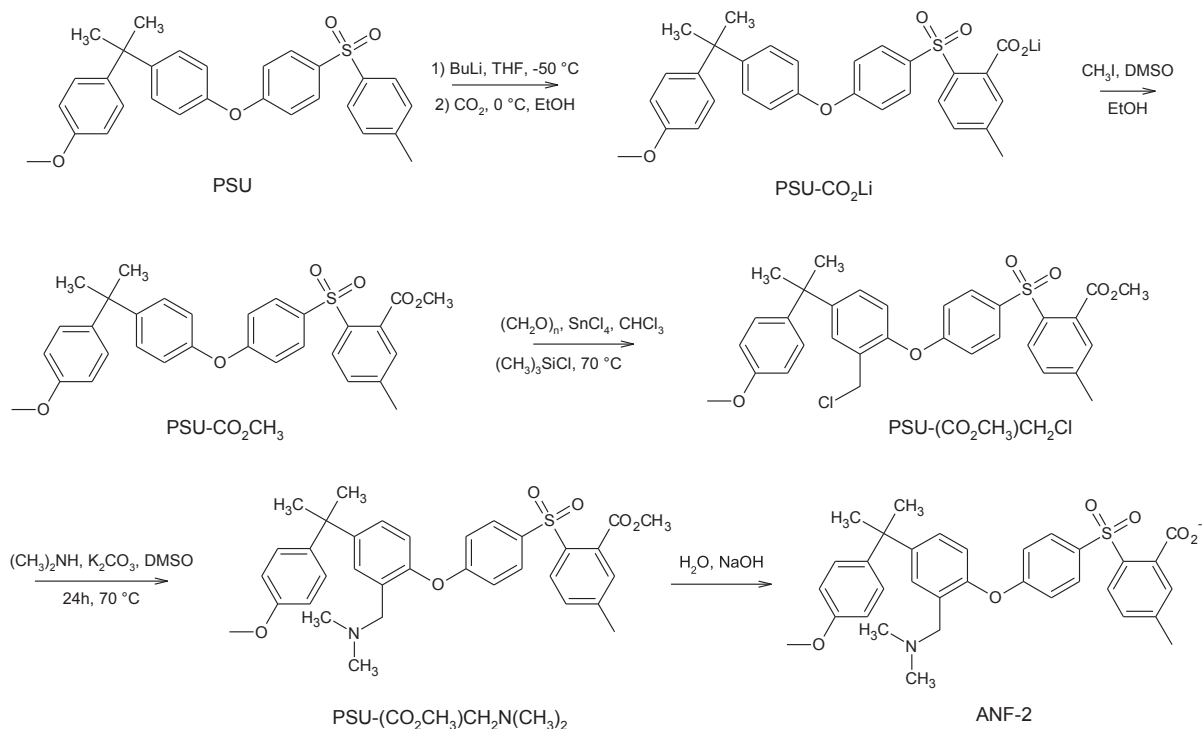


Fig. 2. Reaction pathways for the synthesis of ANF-2.

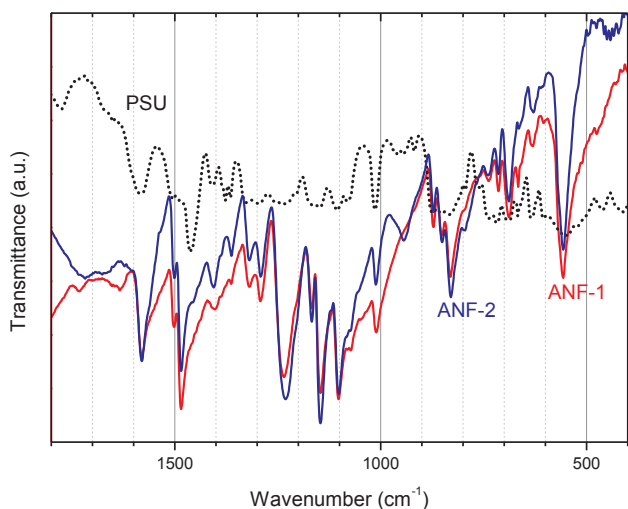


Fig. 3. FTIR spectra of ANF-1 (red), ANF-2 (blue) and PSU (black dots). (For interpretation of the references to colour in this figure legend, the reader is referred to the web version of this article.)

degree was 73%.

For ANF-2, the degree of carboxylation determined by back-titration was DCA = 0.80 and the degree of amination obtained from NMR was DAM = 0.70. We had therefore a slight excess of acidic vs. basic groups. One should underline that the certitude to have equal amounts of acidic and basic is an interesting feature of ANF-1.

Patrickios [48] derived equations relating the isoelectric point and the acid constants, when the number of acidic and basic groups is not identical. The titration of ANF-2 gave an inflection corresponding to an isoelectric point: $\text{pI} = 6.9$. The acid constant determined at half neutralization was $\text{pK}_{\text{a}1} = 4.4$, which is similar to the pK_{a} of benzoic acid ($\text{pK}_{\text{a}} = 4.2$). The calculated $\text{pK}_{\text{a}2}$ of the ammonium group according to Eq. (3) was 9.4, very similar to the pK_{a} of benzylamine (9.34 [49]), corresponding to a basic constant of the amine: $\text{pK}_{\text{b}} = 4.6$. The pK_{a} value for ANF-1 and ANF-2 reflect the general trend observed for aliphatic and aromatic acids: the latter present a higher acidity than the aliphatic ones. The values of amine groups for the two samples were in agreement with the higher basicity of secondary amines. The higher pH of the isoelectric point for ANF-2 respected this trend and was also associated to the slightly higher quantity of the acidic functions.

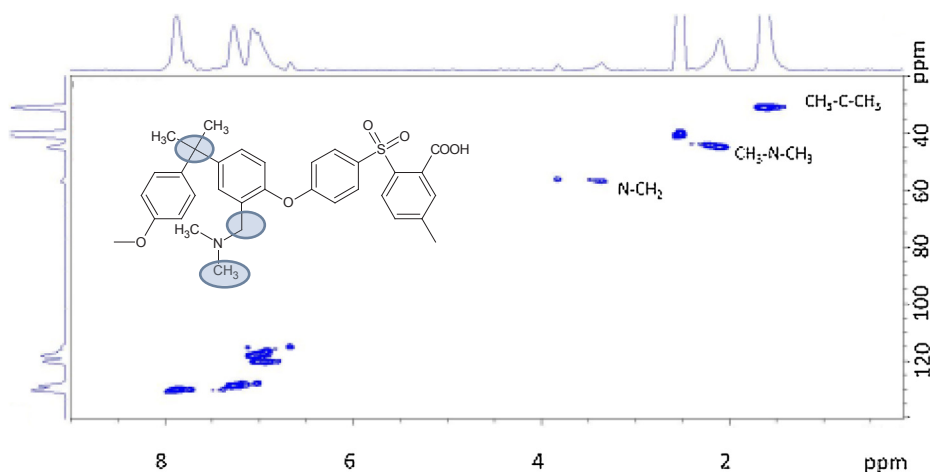


Fig. 4. ^1H - ^{13}C HSQC spectrum of ANF-2.

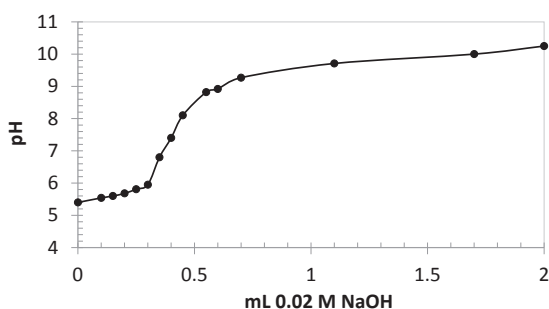


Fig. 5. Acid-base titration of ANF-1.

3.3. Thermogravimetric analysis

The high-resolution thermograms in Fig. 6 showed the different behaviour of the two compounds. The decomposition of ANF-1 started above 330 °C with the loss of ammonium groups together with the complete side chain. The decomposition of ANF-2 occurred in steps with the removal of the carboxylic groups occurring around 250 °C, followed by the loss of the secondary amine around 350 °C. The decomposition of the PSU main chain occurred above 400 °C for both samples. The higher decomposition temperature for ANF-2 was attributed to the formation of macromolecular cross-links as observed in the pyrolysis of carboxylated aromatic polymers [50].

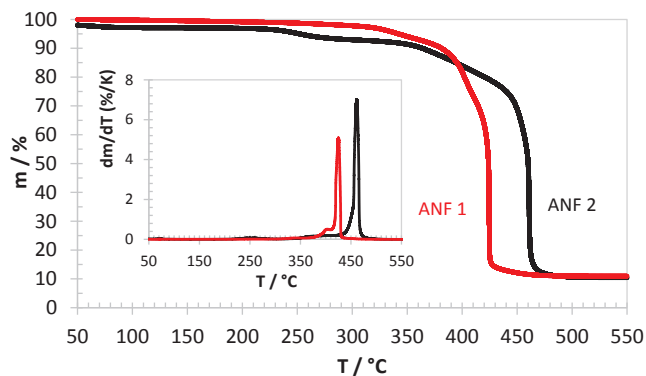


Fig. 6. High-resolution thermogravimetric analysis of ANF-1 (red) and ANF-2 (black). Inlay: derivative curves. (For interpretation of the references to colour in this figure legend, the reader is referred to the web version of this article.)

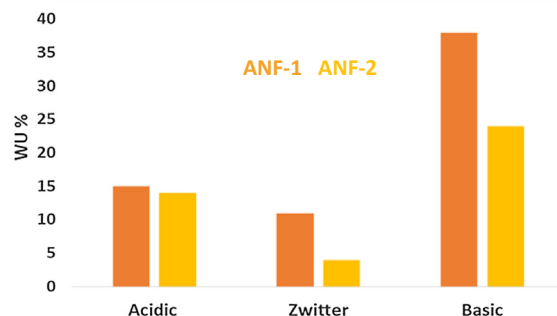
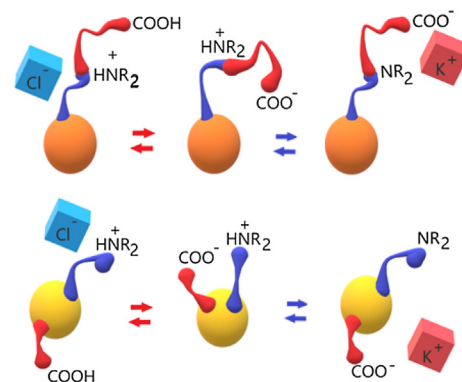


Fig. 7. Acid-base equilibria and water uptake in amphoteric ionomers: top ANF-1 (orange); bottom ANF-2 (yellow). (For interpretation of the references to colour in this figure legend, the reader is referred to the web version of this article.)

3.4. Water uptake and ionic conductivity

The water uptake of acidic, basic and zwitterionic forms of ANF-1 and ANF-2 is reported in Fig. 7. The hydration depends on the ionization of the functional groups. In the acid form, the ionomers are Cl^- conductors, due to the protonation of the amine groups. The dissociation of the carboxylic acid is in fact very low (around 1%). In the basic form, the carboxylic acid is neutralized and the ionomers are K^+ conducting. In the zwitterionic form, the ionic conductivity depends on the distance between ionic groups. If they are near (typically below the distance corresponding to Manning condensation [51]), the ionic groups are undissociated or form ion pairs (such as carboxylate-ammonium). If the distance is larger, both anions and cations can conduct.

The higher water uptake of the basic forms is in agreement with the higher hydration of K^+ and grafted CO_2^- (basic form) in comparison

Table 1
Ionic conductivity σ (through-plane) and activation energy (E_A) of ANF-1 and ANF-2 in acidic, basic and zwitterionic forms.

| T/K | $\sigma/S\text{ cm}^{-1}$ | | | | | |
|----------|---------------------------|---------------------|---------------------|---------------------|---------------------|---------------------|
| | ANF 1 | | | ANF 2 | | |
| | Acidic | Basic | Zwitter | Acidic | Basic | Zwitter |
| 298 | $1.4 \cdot 10^{-6}$ | $1.5 \cdot 10^{-5}$ | $6.2 \cdot 10^{-6}$ | $1.2 \cdot 10^{-6}$ | $5.6 \cdot 10^{-6}$ | $7.2 \cdot 10^{-7}$ |
| 313 | $1.6 \cdot 10^{-6}$ | $3.2 \cdot 10^{-5}$ | $7.8 \cdot 10^{-6}$ | $3.5 \cdot 10^{-6}$ | $1.0 \cdot 10^{-5}$ | $6.2 \cdot 10^{-7}$ |
| 333 | $3.0 \cdot 10^{-6}$ | $4.1 \cdot 10^{-5}$ | $9.5 \cdot 10^{-6}$ | $8.2 \cdot 10^{-6}$ | $2.1 \cdot 10^{-5}$ | – |
| 353 | $3.2 \cdot 10^{-6}$ | $4.5 \cdot 10^{-5}$ | $1.0 \cdot 10^{-5}$ | $1.5 \cdot 10^{-5}$ | $4.4 \cdot 10^{-5}$ | – |
| E_A/eV | 0.16 | 0.17 | 0.09 | 0.41 | 0.34 | – |

with Cl^- and grafted NR_3H^+ (acid form) [38,52]. The zwitterionic form has the lowest water uptake showing a low concentration of free ions. The generally larger water uptake observed for ANF-1 might be attributed to the flexible side chain containing the carboxylic group at the chain end, allowing a better hydrophilic-hydrophobic nanophase separation, as discussed recently [53].

The ionic conductivity of ANF-1 and ANF-2 at various temperatures is reported in Table 1. The ionic conductivity of ANF-2 is in agreement with the expectation: the zwitterionic form shows the lowest value, corresponding to a low amount of mobile ions, whereas the highest conductivity is observed for the basic form containing mobile K^+ ions and presenting the highest water uptake.

We have previously shown the importance of the hydration for the ion conduction, due to the improvement of the ion mobility in the presence of water [54]. The activation energy is slightly lower for the K^+ -conducting basic form, but the values are slightly higher than other cation-and anion-conducting ionomers [55].

The data for ANF-1 are more surprising, because the lowest conductivity is observed for the acidic form, confirmed by several measurements. The activation energies are consistently much below those for ANF-2 and in good agreement with the literature [55,56]. One possible explanation is the presence of a flexible aliphatic side chain, like in Nafion-type ionomers [10].

The low conductivity of the acid form of ANF-1 can be related to the particular structure of the polymer, considering that nitrogen is

protonated and only the anions conduct. It was recently reported that the conductivity of AEM is very dependent on the position where the ammonium groups are grafted and the length of the side chain [57]. Jannasch and co-workers found that ionomers with the ammonium group in benzylic position and a long spacer showed the lowest conductivity which was linked to poor ion cluster formation [53]. Instead, ionomers with ion conducting groups at the end of long side chains presented the highest ion conductivity. We assume that similar effect can justify the low conductivity of the acid form and the large conductivity of the basic form of ANF-1, where the carboxylic group is at the end of the side chain (Fig. 8).

4. Conclusions

In this work, we studied two model cases of amphoteric ionomers: (1) in ANF-1, acid and basic groups were both in the flexible amino acid side chain, (2) in ANF-2, acid and basic groups were separately tethered on the backbone. Hydration and ionic conductivity were dependent on the type and amount of ionic groups and pH-dependent. The basic form, containing fixed carboxylate and mobile K^+ ions, presented the largest water uptake and ion conductivity, especially in the ionomer with the carboxylic group at the end of the side chain, probably due to the best nanophase separation. The acid form of ANF-1, containing ammonium ions in benzylic position and mobile Cl^- ions, presented the lowest conductivity showing the negative effect of the extender chain linked to N^+ , as reported previously for anion exchange polymers. In ANF-2, the lowest conductivity was observed, as expected, for the zwitterionic form. This work emphasised that the properties of amphoteric ionomers were very dependent on the position of the ionic groups.

Data availability

The raw/processed data required to reproduce these findings cannot be shared at this time as the data also forms part of an ongoing study.

Acknowledgments

The research leading to these results received funding from the European Union's Horizon 2020 research and innovation programme

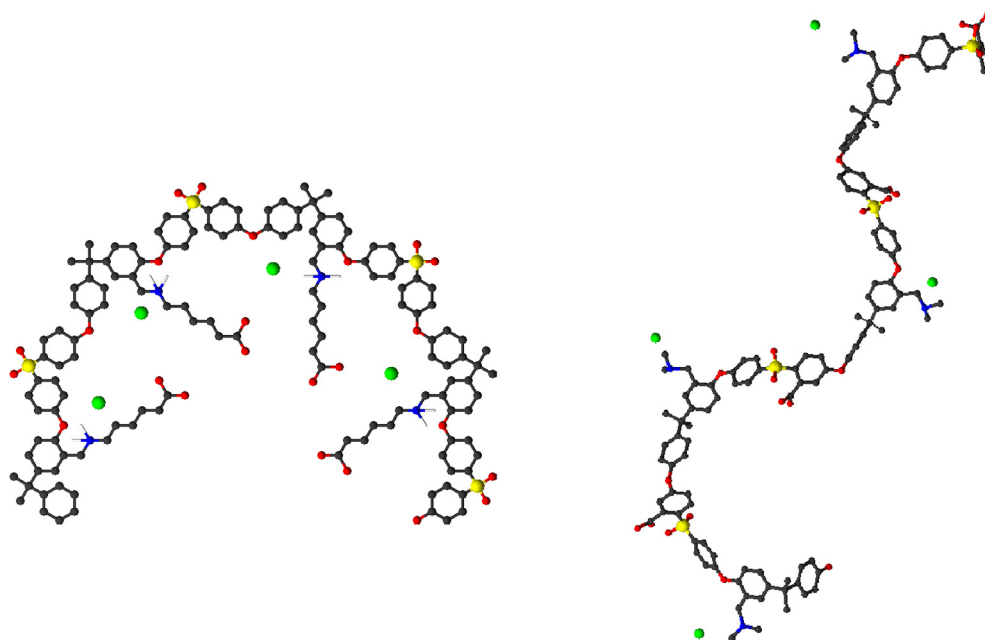


Fig. 8. Schematic representation of the acid form with mobile chlorine ions (green) of: (left) ANF-1 and (right) ANF-2. (For interpretation of the references to colour in this figure legend, the reader is referred to the web version of this article.)

under grant agreement CREATE No. 721065.

Appendix A. Supplementary material

Supplementary data to this article can be found online at <https://doi.org/10.1016/j.eurpolymj.2019.07.001>.

References

- [1] H.P. Gregor, Gibbs-Donnan equilibria in ion exchange resin systems, *J. Am. Chem. Soc.* 73 (2) (1951) 642–650.
- [2] H.P. Gregor, A general thermodynamic theory of ion exchange processes, *J. Am. Chem. Soc.* 70 (3) (1948) 1293–1293.
- [3] M.D. Afonso, M.N. de Pinho, Transport of $MgSO_4$, $MgCl_2$, and Na_2SO_4 across an amphoteric nanofiltration membrane, *J. Membr. Sci.* 179 (1–2) (2000) 137–154.
- [4] M.S. Jyothi, V. Nayak, M. Padaki, R.G. Balakrishna, K. Soontarapa, Aminated polysulfone/ TiO_2 composite membranes for an effective removal of Cr(VI), *Chem. Eng. J.* 283 (2016) 1494–1505.
- [5] F.Q. Xuan, J.S. Liu, Preparation, characterization and application of zwitterionic polymers and membranes: current developments and perspective, *Polym. Int.* 58 (12) (2009) 1350–1361.
- [6] E. Agel, J. Bouet, J.F. Fauvarque, Characterization and use of anionic membranes for alkaline fuel cells, *J. Power Sources* 101 (2) (2001) 267–274.
- [7] K.D. Kreuer, S.J. Paddison, E. Spohr, M. Schuster, Transport in proton conductors for fuel-cell applications: simulations, elementary reactions, and phenomenology, *Chem. Rev.* 104 (10) (2004) 4637–4678.
- [8] J. Jagur-Grodzinski, Polymeric materials for fuel cells: concise review of recent studies, *Polym. Adv. Technol.* 18 (10) (2007) 785–799.
- [9] K.D. Kreuer, Ion conducting membranes for fuel cells and other electrochemical devices, *Chem. Mater.* 26 (1) (2014) 361–380.
- [10] K.A. Mauritz, R.B. Moore, State of understanding of Nafion, *Chem. Rev.* 104 (10) (2004) 4535–4585.
- [11] J. Roziere, D.J. Jones, Non-fluorinated polymer materials for proton exchange membrane fuel cells, *Annu. Rev. Mater. Res.* 33 (2003) 503–555.
- [12] M. Braglia, I.V. Ferrari, T. Djenizian, S. Kaciulis, P. Soltani, M.L. Di Vona, P. Knauth, Bottom-up electrochemical deposition of poly(styrene sulfonate) on nanoarchitectured electrodes, *ACS Appl. Mater. Interfaces* 9 (27) (2017) 22902–22910.
- [13] I.V. Ferrari, M. Braglia, T. Djenizian, P. Knauth, M.L. Di Vona, Electrochemically engineered single Li-ion conducting solid polymer electrolyte on titania nanotubes for microbatteries, *J. Power Sources* 353 (2017) 95–103.
- [14] B. Bauer, H. Strathmann, F. Effenberger, Anion-exchange membranes with improved alkaline stability, *Desalination* 79 (2–3) (1990) 125–144.
- [15] J.R. Varcoe, P. Atanassov, D.R. Dekel, A.M. Herrington, P.A. Kohl, A.R. Kucernak, W.E. Mustain, K. Nijmeijer, K. Scott, T.W. Xu, L. Zhuang, Anion-exchange membranes in electrochemical energy systems, *Energy Environ. Sci.* 7 (10) (2014) 3135–3191.
- [16] M.L. Di Vona, M. Casciola, A. Donnadio, M. Nocchetti, L. Pasquini, R. Narducci, P. Knauth, Anionic conducting composite membranes based on aromatic polymer and layered double hydroxides, *Int. J. Hydrogen Energy* 42 (5) (2017) 3197–3205.
- [17] S.E. Kudaibergenov, N. Nuraje, V.V. Khutoryanskiy, Amphoteric nano-, micro-, and macrogels, membranes, and thin films, *Soft Matter* 8 (36) (2012) 9302–9321.
- [18] H. Matsumoto, Y. Koyama, A. Tanioka, Interaction of proteins with weak amphoteric charged membrane surfaces: effect of pH, *J. Colloid Interface Sci.* 264 (1) (2003) 82–88.
- [19] H. Tamagawa, M. Taya, A theoretical prediction of the ions distribution in an amphoteric polymer gel, *Mater Sci Eng A-Struct Mater Proper Microstruct Process* 285 (1–2) (2000) 314–325.
- [20] N.L. Burns, K. Holmberg, C. Brink, Influence of surface charge on protein adsorption at an amphoteric surface: effects of varying acid to base ratio, *J. Colloid Interface Sci.* 178 (1) (1996) 116–122.
- [21] S.J. Fang, H. Kawaguchi, Colloidal properties and protein adsorption of amphoteric microspheres, *Colloids Surf. A-Physicochem. Eng. Aspects* 211 (1) (2002) 79–84.
- [22] Y.F. Wang, M.S.S. Chow, Z. Zuo, Mechanistic analysis of pH-dependent solubility and trans-membrane permeability of amphoteric compounds: application to sildanafinil, *Int. J. Pharm.* 352 (1–2) (2008) 217–224.
- [23] R. Imboden, G. Imanidis, Effect of the amphoteric properties of salbutamol on its release rate through a polypropylene control membrane, *Eur. J. Pharm. Biopharm.* 47 (2) (1999) 161–167.
- [24] T. Kanamori, M. Fukuda, K. Sakai, Structural-analysis of hemodialysis membranes by evaluating distribution volume of water contained in the membranes, *J. Colloid Interface Sci.* 171 (2) (1995) 361–365.
- [25] P. Fievet, C. Labbez, A. Szymczyk, A. Vidonne, A. Foissy, J. Pagetti, Electrolyte transport through amphoteric nanofiltration membranes, *Chem. Eng. Sci.* 57 (15) (2002) 2921–2931.
- [26] Y. Hirata, G. Sugihara, A. Yamauchi, Transport number of an ion across an amphoteric ion-exchange membrane in $CaCl_2$ -NaCl system, *J. Membr. Sci.* 66 (2–3) (1992) 235–240.
- [27] J. Balster, S. Srinantharajah, R. Sumbharaju, I. Punt, R.G.H. Lammertink, D.F. Stamatiadis, M. Wessling, Tailoring the interface layer of the bipolar membrane, *J. Membr. Sci.* 365 (1–2) (2010) 389–398.
- [28] V. Zabolotsky, S. Utin, A. Bespalov, V. Strelkov, Modification of asymmetric bipolar membranes by functionalized hyperbranched polymers and their investigation during pH correction of diluted electrolytes solutions by electrodialysis, *J. Membr. Sci.* 494 (2015) 188–195.
- [29] R. Zahn, J. Voros, T. Zambelli, Swelling of electrochemically active polyelectrolyte multilayers, *Curr. Opin. Colloid Interface Sci.* 15 (6) (2010) 427–434.
- [30] R. Narducci, L. Pasquini, J.F. Chailan, P. Knauth, M.L. Di Vona, Low-permeability poly(ether ether ketone)-based amphoteric membranes, *Chempluschem* 81 (6) (2016) 550–556.
- [31] F.D. Korosy, Amphoteric ion-permeable membrane, *Desalination* 16 (1) (1975) 85–103.
- [32] P. Knauth, L. Pasquini, M.L. Di Vona, Comparative study of the cation permeability of protonic, anionic and amphoteric membranes, *Solid State Ion.* 300 (2017) 97–105.
- [33] J. Yuan, C.H. Yu, J. Peng, Y. Wang, J. Ma, J.Y. Qiu, J.Q. Li, M.L. Zhai, Facile synthesis of amphoteric ion exchange membrane by radiation grafting of sodium styrene sulfonate and N, N-dimethylaminoethyl methacrylate for vanadium redox flow battery, *J. Polym. Sci. Part A-Polym. Chem.* 51 (24) (2013) 5194–5202.
- [34] E. Sgreccia, L. Pasquini, G. Ercolani, P. Knauth, M. Luisa Di Vona, Stimuli-responsive amphoteric ion exchange polymers bearing carboxylic and amine groups grafted to a cross-linkable silica network, *Eur. Polym. J.* (2019).
- [35] Y.S. Yang, A. Siu, T.J. Peckham, S. Holdcroft, Structural and morphological features of acid-bearing polymers for PEM fuel cells, *Fuel Cells* 1215 (2008) 55–126.
- [36] H.-S. Dang, P. Jannasch, A comparative study of anion-exchange membranes tethered with different hetero-cycloaliphatic quaternary ammonium hydroxides, *J. Mater. Chem. A* 5 (41) (2017) 21965–21978.
- [37] M.L. Di Vona, R. Narducci, L. Pasquini, K. Pelzer, P. Knauth, Anion-conducting ionomers: Study of type of functionalizing amine and macromolecular cross-linking, *Int. J. Hydrogen Energy* 39 (26) (2014) 14039–14049.
- [38] L. Pasquini, M.L. Di Vona, P. Knauth, Effects of anion substitution on hydration, ionic conductivity and mechanical properties of anion-exchange membranes, *New J. Chem.* 40 (4) (2016) 3671–3676.
- [39] R. Narducci, J.F. Chailan, A. Fahs, L. Pasquini, M.L. Di Vona, P. Knauth, Mechanical properties of anion exchange membranes by combination of tensile stress-strain tests and dynamic mechanical analysis, *J. Polym. Sci. Part B-Polym. Phys.* 54 (12) (2016) 1180–1187.
- [40] M.D. Guiver, G.P. Robertson, S. Rowe, S. Foley, Y.S. Kang, H.C. Park, J. Won, H.N.L. Thi, Modified polysulfones. IV. Synthesis and characterization of polymers with silicon substituents for a comparative study of gas-transport properties, *J. Polym. Sci. Part A-Polym. Chem.* 39 (13) (2001) 2103–2124.
- [41] M.L. Di Vona, D. Marani, A. D'Epifanio, E. Traversa, M. Trombetta, S. Licocchia, A covalent organic/inorganic hybrid proton exchange polymeric membrane: synthesis and characterization, *Polymer* 46 (6) (2005) 1754–1758.
- [42] S. Licocchia, M.L. Di Vona, A. D'Epifanio, Z. Ahmed, S. Bellitto, D. Marani, B. Mecheri, C. de Bonis, M. Trombetta, E. Traversa, SPPSU-based hybrid proton conducting polymeric electrolytes for intermediate temperature PEMFCs, *J. Power Sources* 167 (1) (2007) 79–83.
- [43] M.D. Guiver, S. Croteau, J.D. Hazlett, O. Kutovay, Synthesis and characterization of carboxylated polysulfones, *Br. Polym. J.* 23 (1–2) (1990) 29–39.
- [44] D. Lin-Vien, N.B. Colthup, W.G. Fateley, J.G. Grasselli, Chapter 10 - compounds containing $-NH_2$, $-NHR$, and $-NR_2$ groups, in: D. Lin-Vien, N.B. Colthup, W.G. Fateley, J.G. Grasselli (Eds.), *The Handbook of Infrared and Raman Characteristic Frequencies of Organic Molecules*, Academic Press, San Diego, 1991, pp. 155–178.
- [45] L.J. Bellamy, *The Infrared Spectra of Complex Molecules*, Chapman and Hall, London, 1980.
- [46] G. Varsanyi, 3 - Normal vibrations of benzene and its derivatives, in: G. Varsanyi (Ed.), *Vibrational Spectra of Benzene Derivatives*, Academic Press, 1969, pp. 141–393.
- [47] A. Giferri, S. Kudaibergenov, Natural and synthetic polyampholytes, 1(a) theory and basic structures, *Macromol. Rapid Commun.* 28 (20) (2007) 1953–1968.
- [48] C.S. Patrickios, Polypeptide amino-acid-composition and isoelectric point. 1. A closed-form approximation, *J. Colloid Interface Sci.* 175 (1) (1995) 256–260.
- [49] H.K. Hall, Correlation of the base strengths of amines¹, *J. Am. Chem. Soc.* 79 (20) (1957) 5441–5444.
- [50] W.S. Mungall, P.F. Britt, A.C. Buchanan, Thermolysis of a polymer model of aromatic carboxylic acids in low-rank coal, *Abstracts of Papers of the American Chemical Society* 213 (1997) 6-FUEL.
- [51] G.S. Manning, Counterion binding in polyelectrolyte theory, *Acc. Chem. Res.* 12 (12) (1979) 443–449.
- [52] R. Narducci, M.L. Di Vona, P. Knauth, Cation-conducting ionomers made by ion exchange of sulfonated poly-ether-ether-ketone: Hydration, mechanical and thermal properties and ionic conductivity, *J. Membr. Sci.* 465 (2014) 185–192.
- [53] H.S. Dang, P. Jannasch, Exploring different cationic alkyl side chain designs for enhanced alkaline stability and hydroxide ion conductivity of anion-exchange membranes, *Macromolecules* 48 (16) (2015) 5742–5751.
- [54] M.L. Di Vona, L. Pasquini, R. Narducci, K. Pelzer, A. Donnadio, M. Casciola, P. Knauth, Cross-linked sulfonated aromatic ionomers via SO_2 bridges: conductivity properties, *J. Power Sources* 243 (2013) 488–493.
- [55] H.N. Sarode, Understanding ion and solvent transport in anion exchange membranes under humidified conditions, *Colorado School of Mines*, 2015.
- [56] R.W. Kopitzke, C.A. Linkous, H.R. Anderson, G.L. Nelson, Conductivity and water uptake of aromatic-based proton exchange membrane electrolytes, *J. Electrochem. Soc.* 147 (5) (2000) 1677–1681.
- [57] C.X. Lin, X.Q. Wang, E.N. Hu, Q. Yang, Q.G. Zhang, A.M. Zhu, Q.L. Liu, Quaternized triblock polymer anion exchange membranes with enhanced alkaline stability, *J. Membr. Sci.* 541 (2017) 358–366.